

Microwave dielectric heating of drops in microfluidic devices

David Issadore,^a Katherine J. Humphry,^b Keith A. Brown,^a Lori Sandberg,^c David A. Weitz^{ab} and Robert M. Westervelt^{*ab}

Received 12th December 2008, Accepted 2nd March 2009

First published as an Advance Article on the web 19th March 2009

DOI: 10.1039/b822357b

We present a technique to locally and rapidly heat water drops in microfluidic devices with microwave dielectric heating. Water absorbs microwave power more efficiently than polymers, glass, and oils due to its permanent molecular dipole moment that has large dielectric loss at GHz frequencies. The relevant heat capacity of the system is a single thermally isolated picolitre-scale drop of water, enabling very fast thermal cycling. We demonstrate microwave dielectric heating in a microfluidic device that integrates a flow-focusing drop maker, drop splitters, and metal electrodes to locally deliver microwave power from an inexpensive, commercially available 3.0 GHz source and amplifier. The temperature change of the drops is measured by observing the temperature dependent fluorescence intensity of cadmium selenide nanocrystals suspended in the water drops. We demonstrate characteristic heating times as short as 15 ms to steady-state temperature changes as large as 30 °C above the base temperature of the microfluidic device. Many common biological and chemical applications require rapid and local control of temperature and can benefit from this new technique.

Introduction

The miniaturization of the handling of liquid and biological samples has enabled great advances in fields such as drug discovery, genetic sequencing and synthesis, cell sorting, single cell gene expression studies, and low-cost portable medicine.^{1–7} At the forefront of this technology are the micro-fabricated pipes, valves, pumps, and mixers of microfluidics that are leading to integrated lab-on-a-chip devices. These integrated microfluidic devices are causing a paradigm shift in fluid handling that is analogous to what integrated circuit technology did for electronics half of a century ago.⁶ A growing library of elements for lab-on-a-chip systems have been developed in recent years for tasks such as the mixing of reagents, detecting and counting of cells, sorting cells, genetic analysis, and protein detection.^{1–7} There is one function, however, that is crucial to many applications and which has remained a challenge: the local control of temperature. The large surface area to volume ratios found in micrometre-scale channels and the close proximity of microfluidic elements make temperature control in such systems a unique challenge.^{8,9}

Much work has been done in the last decade to improve local temperature control in microfluidic systems. The most common technique uses Joule heated metal wires and thin films to conduct heat into fluid channels.^{10–13} The thermal conductivity of microfluidic devices control the localization of the temperature change and tends to be in the order of centimetres.^{9,11} Temporal control is limited by the heat capacity and thermal coupling of the microfluidic device to the environment and thermal relaxation times tend to be in the order of seconds.^{9,11} Alternative

techniques to improve the localization and response time have been developed, such as those that use non-contact infrared heating of water in glass microfluidic systems¹⁴ and integrated micrometre size Peltier Junctions to transfer heat between two channels containing fluid at different temperatures.¹⁵ Fluids have also been cooled on millisecond time scales with evaporative cooling by pumping gasses into the fluid channels.¹⁶

The focus of our research is to integrate electronics with microfluidics to bring new capabilities to lab-on-a-chip systems.^{6,7} In this paper we present a technique to locally and rapidly heat water in drop based microfluidic systems with microwave dielectric heating. The devices are fabricated using soft lithography and are connected to inexpensive commercially available microwave electronics. This work builds on previous work in which microwaves have been used to heat liquid in microfluidic devices^{17–20} by achieving significantly faster thermal response times and a greater temperature range. In our device, drops of water are thermally isolated from the bulk of the device and this allows exceptionally fast heating and cooling times $\tau_s = 15$ ms to be attained and the drops' temperature to be increased by 30 °C. The coupling of microwave electronics with microfluidics technology offers an inexpensive and easily integrated technique to locally and rapidly control temperature.

Theory of dielectric heating

Dielectric heating describes the phenomenon by which a material is heated with a time-varying electric field. Induced and intrinsic dipole moments within an object will align themselves with a time-varying electric field. The energy associated with this alignment is viscously dissipated as heat into the surrounding solution. The power density P absorbed by a dielectric material is given by the frequency ω of the applied electric field, the loss factor ϵ'' of the material, the vacuum permittivity ϵ_0 , and the electric field strength $|E|$ with the expression:²¹

^aSchool of Engineering and Applied Sciences, Harvard University, Cambridge, MA, 02138, USA. E-mail: westervelt@seas.harvard.edu

^bDepartment of Physics, Harvard University, Cambridge, MA, 02138, USA

^cCollege of Engineering and Applied Sciences, University of Wyoming, Laramie, WY, 82071, USA

$$P = \omega \varepsilon_0 \varepsilon'' |E|^2 \quad (1)$$

The loss factor of the material is dependent on the frequency of the electric field and the characteristic time τ of the dielectric relaxation of the material, with the expression:

$$\varepsilon'' = \frac{(\varepsilon_s - \varepsilon_\infty)\omega\tau}{1 + (\omega\tau)^2} \quad (2)$$

where $\varepsilon_s = 78.4\varepsilon_0$ is the low frequency dielectric constant of water, $\varepsilon_\infty = 1.78\varepsilon_0$ is the optical dielectric constant, and $\tau = 9.55$ ps is the dielectric relaxation time of water at $T = 25^\circ\text{C}$.^{22,23}

Due to water's large dielectric loss at GHz frequencies, microwave power is absorbed much more strongly by water rather than PDMS or glass. Our device operates at 3.0 GHz, a frequency very close to that of commercial microwave ovens (2.45 GHz), that is below the frequency associated with the relaxation time of water but where water still readily absorbs power. It is inexpensive to engineer electronics to produce and deliver 3.0 GHz frequencies because it is near the well-developed frequencies of the telecommunications industry.

Model of dielectric heating of drops

Two independent figures of merit describe the heater, the steady-state change in temperature ΔT_{ss} that the drops attain and the characteristic time τ_s that it takes to change the temperature. The steady-state temperature occurs when the microwave power entering the drop equals the rate that heat leaves the drop into the thermal bath. The thermal relaxation time depends only on the geometry and the thermal properties of the drops and the channel and is independent of the microwave power.

To describe our heater we use a simplified model in which the temperature of the channel walls do not change. The thermal conductivity of the glass and PDMS channel walls is much larger than that of the fluorocarbon (FC) oil in which the drops are suspended, which allow the glass and PDMS mold to act as a large thermal reservoir that keeps the channel walls pinned to the base temperature.

The drop is modelled as having a heat capacity that connects to the thermal reservoir through a thermal resistance. The drop has a heat capacity $C = VC_w$ that connects to the thermal reservoir with a thermal resistance $R = L/Ak_{oil}$, where V is the volume and A is the surface area of the drop, C_w is the heat capacity per volume of water, L is the characteristic length between the drop and the channel wall, and k_{oil} is the thermal conductivity of the oil surrounding the drop. A steady-state temperature ΔT_{ss} is reached when the microwave power PV entering the drop is equal to the power leaving the drop $\Delta T_{ss}k_{oil}A/L$. We find the steady-state temperature $\Delta T_{ss} = PVR$ to be:

$$\Delta T_{ss} = \frac{V}{A} \frac{L}{k_{oil}} P \quad (3)$$

The system has a characteristic time scale $\tau_s = RC$ that describes the thermal response time of the system,

$$\tau_s = \frac{V}{A} \frac{L}{k_{oil}} C_w \quad (4)$$

The characteristic time scale τ_s describes the thermal relaxation time, the time it takes for the drop to reach an equilibrium temperature when the microwave power is turned on and the time that it takes for the drop to return to the base temperature of the device when the microwaves are turned off.

This simplified model describes several key features of the microwave heater. The steady-state temperature is linearly proportional to the microwave power, whereas the characteristic thermal relaxation time is independent of the microwave power. The characteristic time and the steady-state temperature are both proportional to the volume to surface ratio of the drops. A trade-off relation exists between the rate of heating $1/\tau_s$ and the steady-state temperature, whereby a larger volume to surface ratio reduces the thermal relaxation time of the heater but decreases its steady-state temperature for a given microwave power, and vice versa. Similarly an increase in the ratio of the characteristic length between the drop and the channel wall and the thermal conductivity of the oil L/k_{oil} increases the thermal relaxation time and increases the steady-state temperature.

Methods

The devices are fabricated using poly(dimethylsiloxane) (PDMS)-on-glass drop-based microfluidics. A schematic of the device is shown in Fig. 1a. Microwave power is locally delivered *via* metal electrodes that are directly integrated into the microfluidic device and that run parallel to the fluid channel. The drops are thermally insulated from the bulk by being suspended in low thermal conductivity oil. Syringe pumps provide the oil and water at constant flow rates to the microfluidic device. A drop maker and two drop splitters in series create drops that are properly sized for the microwave heater. The microwave power is created off chip using inexpensive commercial components.

Drops are created using a flow-focusing geometry²⁴ as is shown in Fig. 1b. A fluorocarbon oil (Fluorinert FC-40, 3M) is used as the continuous phase and the resulting drops contain 0.1 μM of carboxyl coated CdSe nanocrystal (Invitrogen) suspended in a phosphate buffered saline (PBS) solution. A surfactant comprised of a polyethyleneglycol (PEG) head group and a fluorocarbon tail (RainDance Technologies) is used to stabilize the drops.²⁵ The walls of the microfluidic channels are coated with *Aquapel*[®] (PPG Industries) to ensure that they are preferentially wet by the fluorocarbon oil. Fluid flow is controlled *via* syringe pumps.

To make drops smaller than the channel height, and thus separated from the walls of the channel to ensure adequate thermal isolation, we use drop splitters²⁶ as is shown in Fig. 1c. The drop splitters are designed to break each drop into two drops of equal volume. Passing a spherical drop through two drop splitters in series decreases the radius of a drop by a factor of $(1/2)^{2/3} = 0.63$. Drop splitters allow the device to be made in a single fabrication step, because they remove the necessity of making the drop maker with a channel height smaller than the rest of the device.²⁴

The metal electrodes are directly integrated into the PDMS device using a low-melt solder fill technique.²⁷ The masks for the soft lithography process are designed to include channels for fluid flow and a set to be filled with metal to form electrodes. After inlet holes have been punched into the PDMS and the

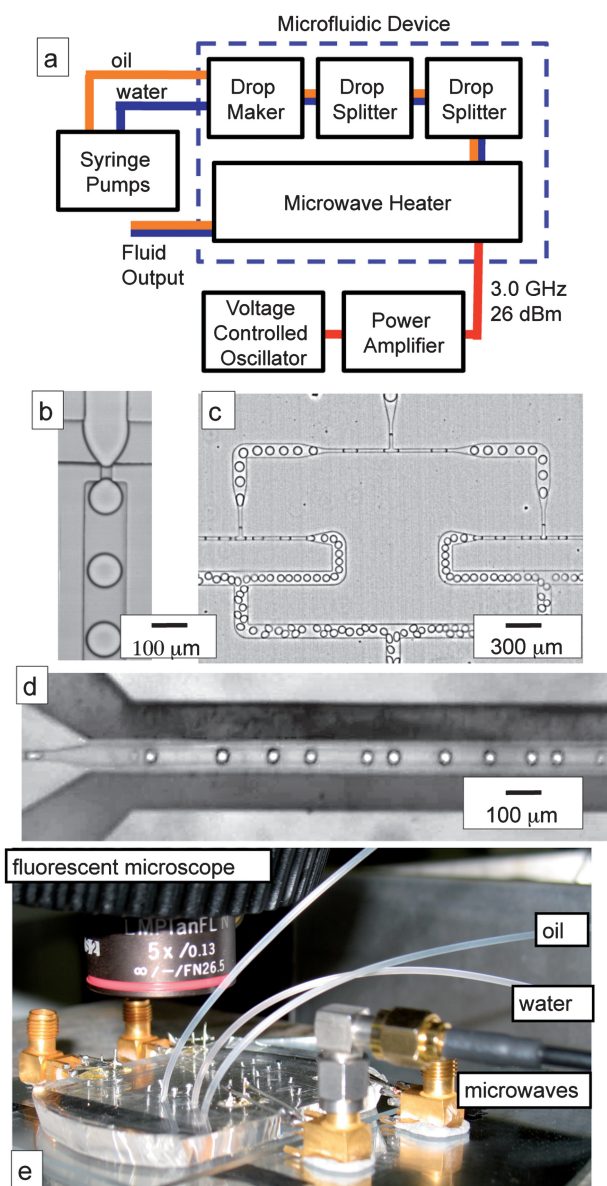


Fig. 1 (a) A schematic of the microwave heating device, showing the oil in orange, the water in blue, and the electronic connections in red, (b) a micrograph of the flow-focusing drop maker, (c) the two sets of drop splitters in series, (d) a micrograph of the microwave heater, the dark regions that run parallel to the fluid channel are the metal lines, (e) a photograph of the microfluidic device, connected to the microwave amplifier with an SMA cable, on top of a hot plate, underneath the fluorescent microscope.

PDMS is bonded to a glass slide, the microfluidic device is placed on a hot plate set to 80 °C. A 0.02 inch diameter indium alloy wire (Indalloy 19; 52% Indium, 32.5% Bismuth, 16.5% Tin from Indium Corporation) is inserted into the electrode channel inlet holes and, as the wire melts, the electrode channels fill with metal *via* capillary action. The resulting electrode channels run along either side of the fluid as is shown in Fig. 1d. To keep the drops from heating from the fringe electric fields before the drop enters the heater the fluid channel is constricted to press the drops against the PDMS wall, which keeps the drops at the same temperature as the base temperature of the microfluidic device.

The electronics that create the microwave power are assembled using inexpensive modules. The microwaves are generated with a voltage controlled oscillator (ZX95-3146-S+, Mini-Circuits) and amplified to a maximum of 11.7 V peak-to-peak with a maximum power of 26 dBm with a power amplifier (ZRL-3500+, Mini-Circuits). The microwave amplifier connects with a cable to a sub miniature assembly (SMA) connector mounted next to the microwave device as is shown in Fig. 1e. Copper wires approximately 2 mm in length connect the SMA connector to the metal electrodes in the PDMS device. Our electronics operate at 3.0 GHz where water's microwave power absorption is roughly 1/3 as efficient as at the frequency associated with water's relaxation time (~18 GHz) but where electronics are inexpensive and commercially available. The electronics used in our system costs less than \$US 200 and are easy to setup.

Finite element simulations are performed to determine the electric field strength in the microwave heater which is used to calculate the microwave power absorbed by the drops. Figure 2

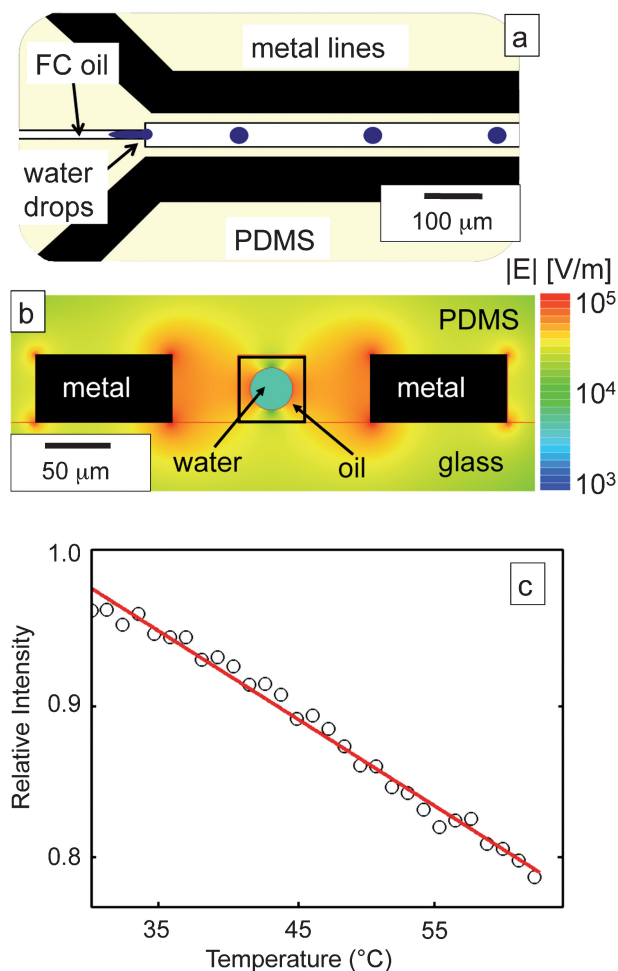


Fig. 2 (a) A schematic of the microwave heater. The black lines represent the metal lines which are connected to the microwave source, the center fluid channel carries drops of water immersed in fluorocarbon (FC) oil, (b) a cross section of the microwave heater with a quasi-static electric field simulation superimposed is shown, the electric field is plotted in log scale, (c) the calibration curve of the CdSe nanoparticles which are used as temperature sensors, where the circles are data points and the red line is the fit.

shows a schematic cross-section of the microfluidic device where the drops pass between the metal electrodes. The channel cross-section has dimensions $50 \times 50 \mu\text{m}^2$. Parallel to and $20 \mu\text{m}$ away from each side of the fluid channel are metal lines that are $100 \mu\text{m}$ wide and $50 \mu\text{m}$ high. Superimposed on the schematic in Fig. 2b is a quasi-static electric field simulation of the electric field (Maxwell, Ansoft). We find that for a 12 V peak-to-peak signal across the metal lines, the RMS electric field within a drop with a $15 \mu\text{m}$ radius suspended in fluorocarbon oil is $|E| \sim 8 \times 10^3 \text{ V m}^{-1}$. The electric field linearly scales with the voltage across the metal lines which allows us to calculate the field within the drop for any voltage. The simulated electric field is combined with eqn (1) and eqn (2) to calculate the microwave power that enters the drops which may be combined with eqn (3) to predict steady-state temperature changes.

The temperature change of the drops is measured remotely by observing the temperature-dependent fluorescence of CdSe nanocrystals suspended in the drops.²⁸ To calibrate our thermometer, we turn the microwave power off and use a hot plate to set the temperature of the microfluidic device. The fluid channel is filled with CdSe nanocrystals suspended in water and the temperature of the hot plate is slowly increased from $25 \text{ }^\circ\text{C}$ to $58 \text{ }^\circ\text{C}$ while the fluorescence intensity of the CdSe quantum dots is measured. The measured fluorescence intensity is plotted as a function of temperature in Fig. 2c. We fit a line with slope $0.69\% \text{ }^\circ\text{C}^{-1} \pm 0.03\% \text{ }^\circ\text{C}^{-1}$ to the data and use this relationship to convert fluorescence measurements into measurements of the change in temperature. A line is fit to the data using a least-squares technique and the error is the uncertainty in the coefficient of the fit. A calibration curve is taken immediately before an experiment. There is no evidence that the CdSe nanoparticles leak from the drops into the oil or precipitate onto the microfluidic channel. We check the microfluidic channel after the experiments and the oil in the waste line and there is no measured fluorescent signal. The device is monitored with an Hamamatsu ORCA-ER cooled CCD camera attached to a BX-52 Olympus microscope. Images are taken with MicroSuite Basic Edition by Olympus and analysed in MATLAB (The MathWorks, Inc.). The microfluidic device is connected with an SMA to the microwave amplifier and sits on top of a hot plate underneath the microscope as is shown in Fig. 1d.

We test our devices by measuring the temperature change of water drops as they travel through the microwave heater. A long-exposure fluorescence image of many drops traveling through the microwave heater shows the ensemble average of the temperature change of drops at each point in the channel. A plot of the drop heating in time may be extracted from this image using the measured flow rate of the drops through the microfluidic system. An experiment is performed with the constant volumetric flow rate of the water at $15 \mu\text{L h}^{-1}$ and the oil at $165 \mu\text{L h}^{-1}$. A bright field, short shutter speed image is taken of the drops traveling through the microwave heater and the drops' average diameter is measured to be $35 \mu\text{m}$. The microwave heater is turned on with a frequency of 3.0 GHz and a peak to peak voltage of 11 V. A long exposure (2 s) fluorescent image is taken of the microwave heater that is normalized against images taken with the microwaves turned off to remove artifacts that arise from irregularities in the geometry of the channel, the light source, and the camera.

Results

The drops are heated to a steady-state temperature change ΔT_{ss} as they pass through the microwave heater. Fig. 3a shows the normalized fluorescence intensity of the drops as they enter the microwave heater superimposed onto a bright-field image of the device. It can be seen that as the drops enter the channel their average fluorescent intensity drops which shows that they are being heated. A line average of the normalized image is taken in the direction perpendicular to the fluid flow and is plotted against the length of the channel, as in Fig. 3b. As the drops are heated the average fluorescent intensity of the drops falls exponentially with distance to 85% of its initial intensity after a path length of $300 \mu\text{m}$. The fluorescent intensity measures the temperature change of the drops, and so we know that drops are heated in a characteristic length of $300 \mu\text{m}$.

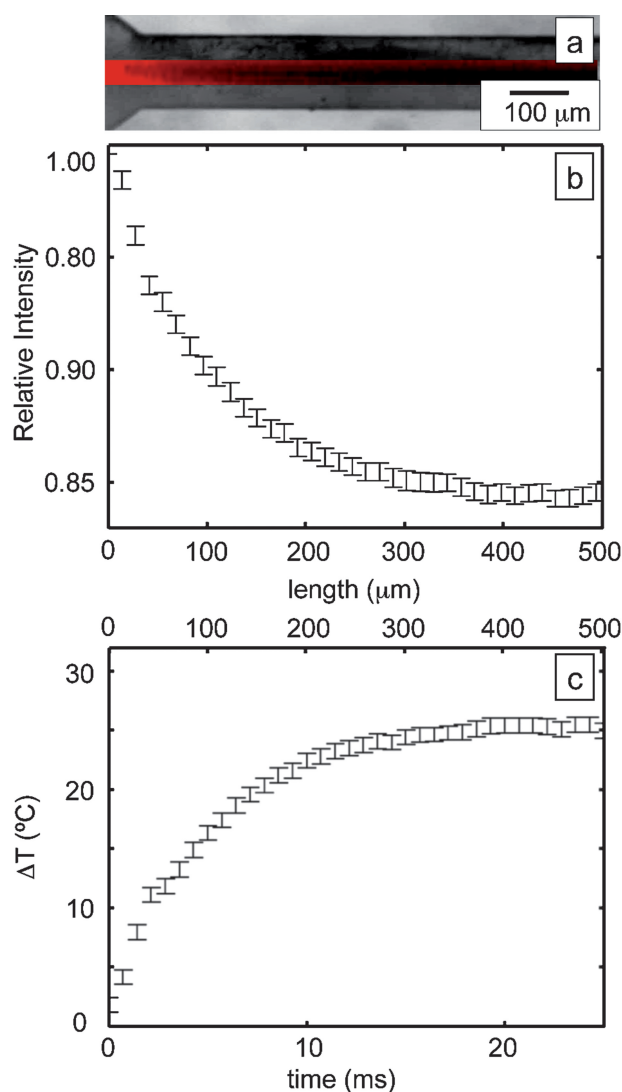


Fig. 3 (a) A 2 s exposure of the fluorescent signal normalized to an image taken with the microwave source turned off superimposed onto a bright field image of the device, (b) the line average of the normalized intensity plotted *versus* distance down the channel, (c) the temperature change ΔT plotted *versus* time and *versus* the distance the drops have traveled down the channel.

The drops are heated to steady-state temperature changes ΔT_{ss} to as much as 30 °C above the base temperature of the microfluidic device in only $\tau_s = 15$ ms. The average temperature change of the drops as a function of time and distance traveled is plotted in Fig. 3c. For this heating power, the temperature rises to a steady-state value of 26 °C above the base temperature of 21 °C in 15 ms. We arrive at the curve in Fig. 3c by using the calibration curve of the CdSe nanocrystals, Fig. 2c, to convert the fluorescent intensity in Fig. 3b into a change in temperature ΔT . The sum of the flow rates of the oil and water are used to calculate the speed of the drops through the channel, which may be used to transform the length in Fig. 3a into the time that the drops have spent in the heater. Each data point consists of the average of 20 independently taken 2 s exposures. The combined statistical error of the measurement of the heating is also plotted in Fig. 3c. The average error is ~ 1.4 °C. We find that the statistical error in the steady-state temperature comes primarily from variations in the size of the drops. The steady-state temperature change of each drop is linearly related to the volume-to-area ratio of the drop and to the distance of the drop to the channel walls, as is described in eqn (3). By observing the drops exit the microwave heating region of the chip, we find that the drops cool with a characteristic time similar to the heating time. In addition, by narrowing the channel at the exit of the microwave heater, the drops are brought closer to the channel wall and the drops return to the base temperature of the oil in less than 1 ms.

The steady-state temperature change ΔT_{ss} of the drops may be set from 0 °C to 30 °C by varying the applied microwave power as is described in eqn (3). The microwave power is controlled by experimentally varying the peak-to-peak voltage of the applied microwave voltage which varies the strength of the electric field inside the drops as is described by our simulations. A series of plots of the change in temperature *versus* time for different applied powers is shown in the inset of Fig. 4a, and shows steady-state temperature changes ranging from 2.8 °C to 30.1 °C, with an average error of 1.5 °C. It is noteworthy that all of the heating curves have an exponential form and have the same characteristic rise time $\tau_s = 15$ ms.

We compare the steady-state temperature changes observed in Fig. 4a for different applied microwave powers with our model of microwave heating and find good agreement. The steady-state temperature change is plotted *versus* the microwave power density in Fig. 4a and is fit with a line. As is expected from eqn (3) the steady-state temperature change rises linearly with applied microwave power. We calculate the microwave power density using the electric field values determined from simulations (Fig. 2b). The only variable in eqn (3) that we do not measure or that is not a material property is L the characteristic length scale between the drop and the channel wall. We estimate this characteristic length $L = 28 \mu\text{m}$ using the measured steady-state temperature change (Fig. 4a) and the known material properties using eqn (3).

We compare the observation that the temperature change approaches steady-state exponentially in time in Fig. 4b with our model of microwave heating and find good agreement. To compare the model's prediction that the drops approach equilibrium exponentially in time with a single relaxation time constant (eqn (4)) with our observations, we plot the change in temperature ΔT subtracted from the steady-state change in temperature ΔT_{ss} *versus* time on a semi-log plot and fit with

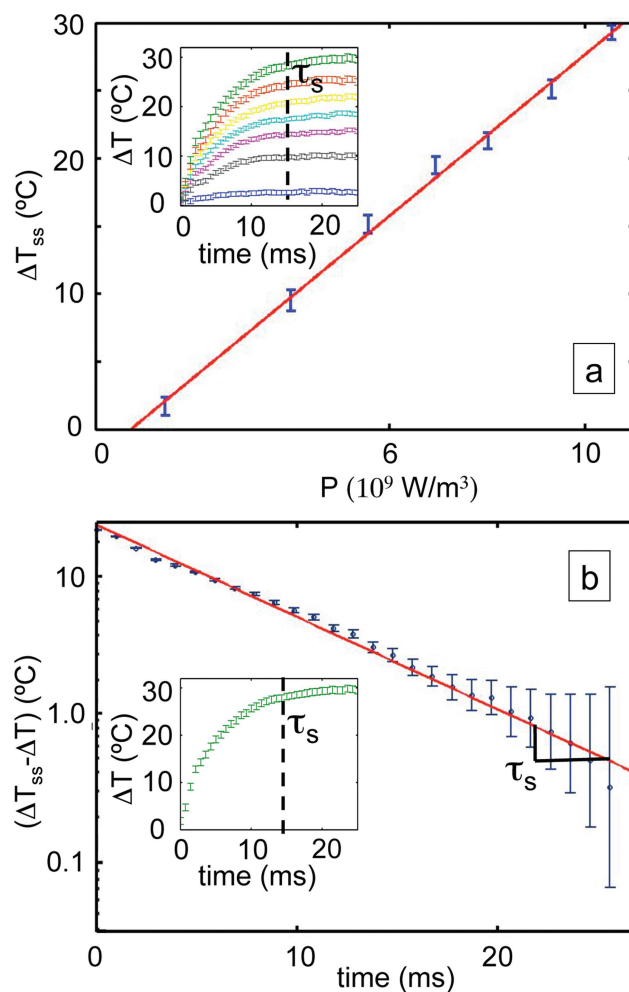


Fig. 4 (a) The steady-state temperature change of the drops is controlled by varying the amplitude of the microwave voltage. In the inset the green curve shows the drop heating *versus* time for microwaves with an amplitude of 11.7 V, the red 11.0 V, the yellow 10.3 V, the light blue 9.3 V, the purple 8.5 V, the grey 7.5 V, and the dark blue 4.5 V. The steady-state temperature change is plotted *versus* the power density, as calculated by eqn (1), in the main plot, (b) the magnitude of the change in temperature ΔT subtracted from the maximum change in temperature ΔT_{ss} *versus* time is plotted on a log-linear scale. The temperature rises as a single exponential with a characteristic time, $\tau_s = 14.7 \pm 0.56$ ms. The inset shows the temperature change *versus* time plot from which the log-linear plot is taken.

a line. As is predicted by our model the drops approach equilibrium exponentially and with a single time constant. The thermal relaxation time constant is measured to be $\tau_s = 14.7 \pm 0.6$ ms. The only variable in eqn (4) that we do not measure is the characteristic length L between the drop and the channel wall. We estimate this characteristic length $L = 35 \mu\text{m}$ using the measured characteristic time constant and known material properties using eqn (4). The independent measurements of the thermal relaxation time and the steady-state temperature change *versus* power give two independent measures of the length L that are within 20% of each other. The difference in the two predictions of L can be at least partially explained by noting that the heat capacity in eqn (4) is larger than we calculate it to be, due to the fact that the channel walls are not a perfect heat sink as our model

assumes. The agreement between the two independent measurements supports our simple model for microwave heating of drops.

Discussion

We have demonstrated an integrated microfluidic microwave dielectric heater that locally and rapidly increases the temperature of drops of water in oil. The large absorption of microwave power by water relative to oil, glass, and PDMS allows local and rapid heating in microfluidic devices without difficult fabrication. Both improving the insulation of drops from the channel walls and increasing the volume to surface area ratio of the drops would allow for larger temperature changes. The statistical error in the steady-state temperature of the drops can be improved by reducing variations in the drop size that arise from fluctuations in the flow from the syringe pumps.

Microwave dielectric heating of drops is well suited for integration with hybrid integrated circuit (IC)/microfluidic systems.^{6,7} Dielectrophoresis chips use arrays of $11 \times 11 \mu\text{m}^2$ electrodes to trap and move drops or cells inside a microfluidic chamber.⁷ If electrodes on the chip can be driven with voltages at GHz frequencies, then one can use the chip to locally heat single drops using the technique outlined in this paper. Chip based thermal control on pL drops would prove to be a valuable tool for a number of applications, including DNA analysis.⁶

Microwave dielectric heating has many exciting scientific and technological applications. One noteworthy potential application for rapid, localized heating in microfluidic devices is PCR.^{11–16} Our heater can raise the temperature of drops up to 30 °C above the base temperature of the oil in which the drops are suspended. By setting the base temperature of the oil in our device to 65 °C and appropriately setting the microwave power, a 30 °C change in temperature could cycle the temperature from 65 °C to 95 °C as required for PCR. Drop-based PCR, which would be especially well suited for our technique, allows for the rapid analysis of large populations of genes and enzymes. Our technique might also be used to set temperatures rapidly and controllably in biological and chemical assays, such as for protein denaturing studies²⁹ and enzyme optimization assays,³⁰ where observations of thermal responses are made on the millisecond time scale.

Acknowledgements

We would like to acknowledge generous support from the Harvard-MIT Center for Cancer Nanotechnology Excellence (CCNE), the Department of Defense (DoD) through the National Defense Science & Engineering Graduate Fellowship (NDSEG) Program, the National Science Foundation (NSF) through the Research Experience for Undergraduates (REU) program, and NSF grants (DMR-0602684 and DBI-0649865), and the Harvard Materials Research Science and Engineering Center at Harvard (DMR-0820484).

References

- 1 G. M. Whitesides, E. Ostuni, S. Takayama, X. Jiang and D. Ingber, *Annu. Rev. Biomed. Eng.*, 2001, **3**, 335, and references therein.
- 2 H. A. Stone, A. D. Stroock and A. Ajdari, *Annu. Rev. Fluid Mech.*, 2004, **36**, 381, and references therein.
- 3 P. Tabeling, *Introduction to Microfluidics*, Oxford University Press, 2005, and references therein.
- 4 P. Yager, T. Edwards, E. Fu, K. Helton, K. Nelson, M. R. Tam and B. H. Weig, *Nature*, 2006, **442**, 412.
- 5 A. W. Martinez, S. T. Phillips, B. J. Wiley, M. Gupta and G. M. Whitesides, *Lab Chip*, 2008, **8**, 2146.
- 6 H. Lee, D. Ham and R. M. Westervelt eds. *CMOS Biotechnology*, Springer, New York, 2007.
- 7 T. P. Hunt, D. Issadore and R. M. Westervelt, *Lab Chip*, 2008, **8**, 81.
- 8 G. Maltezos, M. Johnston and A. Scherer, *Appl. Phys. Lett.*, 2005, **87**, 154105.
- 9 J. Lee and I. Mudawar, *Int. J. Heat Mass Transfer*, 2005, **48**, 928.
- 10 H. Nakano, K. Matsuda, M. Yohda, T. Nagmune, I. Endo and T. Yamane, *Biosci. Biotechnol. Biochem.*, 1994, **58**, 349.
- 11 E. T. Lagally, P. C. Simpson and R. A. Mathies, *Sens. Actuators*, 2000, **B63**, 138.
- 12 J. Liu, M. Enzelberger and S. R. Quake, *Electrophoresis*, 2002, **23**, 1531.
- 13 J. Khandurina, T. E. McKnight, S. C. Jacobson, L. C. Waters, R. S. Foote and J. M. Ramsey, *Anal. Chem.*, 2000, **72**, 2995.
- 14 R. P. Oda, M. A. Strausbauch, A. F. R. Huhmer, N. Borson, S. R. Jurens, J. Craighead, P. J. Wettstein, B. Eckloff, B. Kline and J. P. Landers, *Anal. Chem.*, 1998, **70**, 4361.
- 15 G. Maltezos, M. Johnston and A. Scherer, *Appl. Phys. Lett.*, 2005, **87**, 154105.
- 16 G. Maltezos, A. Rajagopal and A. Scherer, *Appl. Phys. Lett.*, 2006, **89**, 074107.
- 17 J. J. Shah, S. G. Sundaresan, J. Geist, D. R. Reyes, J. C. Booth, M. V. Rao and M. Gaitan, *J. Micromech. Microeng.*, 2007, **17**, 2224.
- 18 S. G. Sundaresan, B. J. Polk, D. R. Reyes, M. V. Rao and M. Gaitan, *Proc. Micro Total Anal. Syst.*, 2005, **1**, 657–659.
- 19 A. Sklavounos, D. J. Marchiarullo, S. L. R. Barker, J. P. Landers and N. S. Barker, *Proc. Micro Total Anal. Syst.*, 2006, **2**, 1238.
- 20 J. Geist, J. J. Shah, M. V. Rao and M. Gaitan, *J. Res. Natl. Inst. Stand. Technol.*, 2007, **112**, 177.
- 21 N. E. Bengtsson and T. Ohlsson, *Proc. IEEE*, 1974, **62**, 44.
- 22 J. N. Murrell, A. D. Jenkins, *Properties of Liquids and Solutions*, 2nd edn, John Wiley & Sons, Chichester, England, 1994.
- 23 The dielectric loss factor is affected by the conductivity of the solution σ , which depends on the concentration of electrolytes.^{17,22} The conductivity leads to a correction $\sigma/\epsilon_0\omega$ that is added to the dielectric loss. At the frequency $f = 3$ GHz used in this paper, the correction is a $\approx 10\%$ change to the loss factor and does not affect the conclusions of this paper.
- 24 S. L. Anna, N. Bontoux and H. A. Stone, *Appl. Phys. Lett.*, 2003, **82**, 364.
- 25 C. Holtze, A. C. Rowat, J. J. Agresti, J. B. Hutchison, F. E. Angile, C. H. H. Schmitz, S. Koester, H. Duan, K. J. Humphry, R. A. Scanga, J. S. Johnson, D. Pisigano and D. A. Weitz, *Lab Chip*, 2008, **8**, 1632.
- 26 D. R. Link, S. L. Anna, D. A. Weitz and H. A. Stone, *Phys. Rev. Lett.*, 1994, **92**, 54503.
- 27 A. C. Siegel, S. S. Shevkoplyas, D. B. Weibel, D. A. Bruzewicz, A. W. Martinez and G. M. Whitesides, *Angew. Chem.*, 2006, **45**, 6877.
- 28 H. Mao, T. Yang and P. S. Cremer, *J. Am. Chem. Soc.*, 2002, **124**, 4432–4435.
- 29 H. F. Arata, F. Gillot, T. Nojima, T. Fujii and H. Fujita, *Lab Chip*, 2008, **8**, 1436–1440.
- 30 D. E. Robertson and B. A. Steer, *Curr. Opin. Chem. Biol.*, 2004, **8**, 141.